Preprint Title Unipolar magnetic field pulses as an advantageous tool for ultrafast spin-flip in superconducting Josephson “atoms”

Authors Daria V. Popolitova, Nikolay V. Klenov, Igor I. Soloviev, Sergey V. Bakurskiy and Olga V. Tikhonova

Article Type Full Research Paper

ORCID® iDs Nikolay V. Klenov - https://orcid.org/0000-0001-6265-3670

Unipolar magnetic field pulses as an advantageous tool for ultrafast spin-flip in superconducting Josephson "atoms"

Daria V. Popolitova[1], Nikolay V. Klenov*[1,2,3], Igor I. Soloviev[2,3], Sergey V. Bakurskiy[2,3], and Olga V. Tikhonova[1,2]

Address: [1]Lomonosov Moscow State University Physics Department, Moscow, 119991, Russia; [2]Lomonosov Moscow State University Skobeltsyn Institute of Nuclear Physics, Moscow, 119991, Russia and [3]All-Russian Research Institute of Automatics n.a. N.L. Dukhov (VNIIA), 127055, Moscow, Russia

Email: Nikolay V. Klenov – nvklenov@gmail.com

* Corresponding author

Abstract

Theoretical approach to consistent fully quantum description of the ultrafast population transfer and magnetization reversal in superconducting meta-atoms induced by picosecond unipolar pulses of magnetic field is developed. A promising scheme based on the regime of stimulated Raman Λ-type transitions between qubit spin states via upper-lying levels is suggested in order to provide an ultrafast spin-flip on the picosecond time scale. The experimental realization of the ultrafast control of circuit -on -chip is presented.

Keywords

quantum-state-control; adiabatic superconducting logic; superconducting qubits, ultrafast spin-flip, Josephson “atoms”.

Introduction

One of the main problems of modern quantum physics is transfer and storage of quantum information. For this reason to develop quantum logic protocols using the fast state control of promising qubits and registers is of great importance. Superconducting artificial atoms based on Josephson junction circuits underlie a number of developments in algorithmic and adiabatic quantum computers, artificial metamaterials, and quantum neural networks. Hence, they seem to be very promising for studies of novel types of fast quantum-state control or initialization [1-15]. In this work, we pay special attention to the search for fundamental possibilities of increasing the speed of dynamic processes in "magnetic" meta-atoms with “controlled” selection rules.

Indeed, in the case when the resonance carrier (“filled”) pulses are used for state preparation and control, the characteristic Rabi-period appears to be in the nanosecond range, which is caused by the small energy separation and near-degeneracy of the atomic levels. For this reason an important task is to decrease the time of the transitions between the spin-states of the meta-atoms (qubits, qutrits, quantum neurons, see Fig. 1) to improve the speed of quantum logic operation. One of the possible ways to solve this problem is to use the unipolar pulses of magnetic field with picosecond duration and almost rectangular envelopes that seem to be very attractive due to their broad frequency spectrum with pronounced near-zero components. The possibilities to control the superconducting qubits (as well as to read their states out) and to induce the Rabi-oscillations by using trains of such pulses with different repetition period were shown in [16-28]. However, because of broad spectrum such unipolar pulses give rise to the transitions not only between the two lowest (“spin qubit”) states but also induce the transitions to the upper levels of the effective Hamiltonian of the magnetic meta-atom. As a result it is difficult to transfer the total population from one spin-state to another and provide totally the spin-flip operation with the efficiency equal to 1.

In this paper we suggest a method of ultrafast control of the population dynamics in superconducting meta-atom by the unipolar pulses using the regime of stimulated Raman Λ-type transitions between “spin qubit” states via upper-lying levels. The possibility to perform the spin-flip and to inverse magnetization on the picosecond scale and even faster is demonstrated. The advantages of the unipolar pulses working in the Λ-type configuration in comparison to direct spin transitions are established. The experimental realization of the theoretically developed scheme is worked out and described.

This paper is organized as follows. In the next Section we present our model and discuss the developed theoretical approach. In the Section “Results and Discussion” we firstly show the theoretical results obtained for the scheme with blocked direct transitions between qubit spin states and demonstrate ultrafast Raman Λ-type spin-flip stimulated by unipolar magnetic pulse (first subsection), then we analyze the interaction of the superconducting meta-atom with the unipolar pulse for allowed direct spin transition and show this case to be non-relevant (second subsection) and finally we present the experimental realization of our suggested promising scheme (third subsection). At the end we give the Conclusions.

Model and theoretical approach

To be specific, we will consider a superconducting ring with three Josephson junctions (see inset in Fig. 1) as a magnetic meta-atom. The potential energy of the system takes the double-well form when the characteristic Josephson energies of the three elements are E_{Jos}, E_{Jos} and αE_{Jos}, α >0.5. We can apply magnetic fluxes Φ_X and Φ_Z in order to control the barrier height and potential asymmetry respectively. Below, we show that in this way we can control the speed of transition between individual states, what is extremely important for the concept presented here.

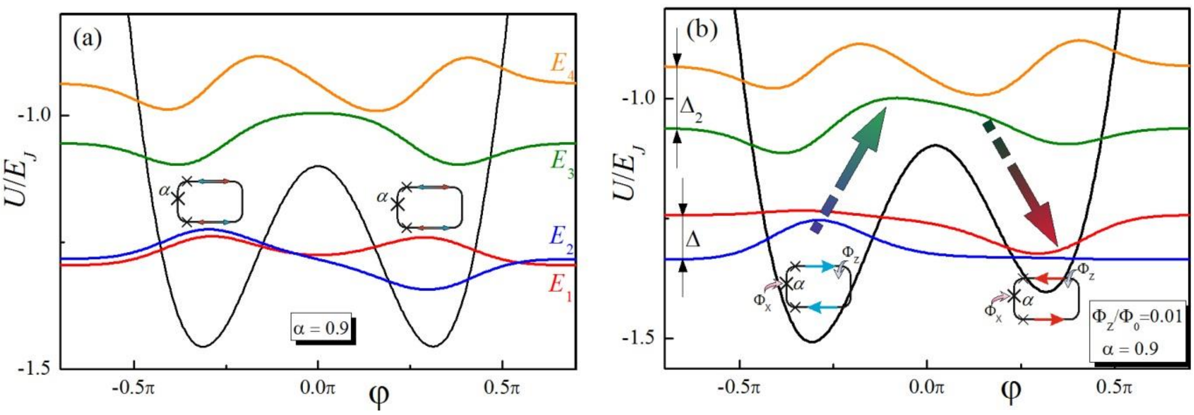

Figure 1: (a) The potential energy and the eigenfunctions (with energies E_1 ,E_2, E_3, E_4) or the three-junction qubit (described in Ref. [3]), where Josephson energies of the elements are E_{Jos}, E_{Jos} and αE_{Jos} (α = 0.9). The characteristic Josephson energy E_{Jos} is 80 times larger than the characteristic Coulomb energy of the heterostructures. φ is the generalized coordinate associated with the Josephson junction phases.

(b) Spin-flip in a double-well potential of the flux-driven superconducting meta-atom (α = 1.5) is shown as a transition between the states with certain values of the magnetic moment (these states correspond to the energy levels of E_1 and E_2, respectively). Applied magnetic flux, Φ_Z, is equal to 0.01 of the magnetic flux quantum, Φ_0. We present here illustrations of the notation used in the text: E_1, E_2, E_3, E_4, Δ, Δ_2.

The dynamics of such superconductive system in a magnetic pulse field is described by the non-stationary Schroedinger equation:

$$i\hbar\frac{\partial\psi}{\partial t} = \left(\hat{H}_0 - \vec{\mu}\vec{H}\right)\psi \tag{1}$$

where $\hat{H}_0$ stands for the unperturbed Hamiltonian of the system, $\vec{H}$ is the external magnetic field and $\vec{\mu}$ stands for the operator of the magnetic moment. In our approach firstly we take into account 3 energy states of such artificial Josephson atom: two spin qubit states with energies E_1, E_2 and one upper-lying level with energy E_3 (see Fig. 1).

The external magnetic field $\vec{H}$ is chosen as unipolar rectangular pulse of duration τ and amplitude A. The key point of our approach is to tune parameters of the meta-atom and the control circuits in order to apply the magnetic field in a proper way to block the direct transitions between the qubit spin states and to allow the Raman Λ-type transitions between them via upper level. Using existing analogy with spin states |↓> and |↑> the direction of $\vec{H}$ should be chosen along the z-axis such as the interaction term $\mu_z H_z$ is proportional to the $\hat{\sigma}_z$ matrix which prevents the direct spin-flip transition.

Finally we expand the non-stationary wave function of the system in terms of the considered eigenfunctions of the double-well potential φ_n with energies E_n :

$$\psi(t) = \sum_n C_n(t)\,\varphi_n \tag{2}$$

and obtain a set of coupled differential equations for the probability amplitudes $C_n(t)$ of the corresponding states with direct spin transition |1>→ |2> being blocked:

$$\begin{cases} i\hbar\dot{C}_1 = \mu_{13}C_3A + C_1E_1 \\ i\hbar\dot{C}_2 = \mu_{23}C_3A + C_2E_2 \\ i\hbar\dot{C}_3 = \mu_{32}C_2A + \mu_{31}C_1A + C_3E_3 \end{cases} \tag{3}$$

Here μ_{ij} stand for the magnetic matrix elements of the allowed transitions and for simplicity we suppose all of them to be of the same value: $\mu_{31}\sim\mu_{32}\sim\mu\sim 10^6\ a.u.$

Further we'll solve the system (3) under the initial condition $C_1 = 1$ which corresponds to the initial population of the lowest spin state. The time-dependent populations of any of considered states can be calculated as following: $W_i = |C_i(t)|^2$. The obtained dynamics of the system is compared to that calculated in the case when the transitions between all the considered states are allowed and found as solution of the following system of equations:

$$\begin{cases} i\hbar\dot{C}_1 = C_1E_1 + \mu_{13}C_3A + \mu_{12}C_2A \\ i\hbar\dot{C}_2 = C_2E_2 + \mu_{23}C_3A + \mu_{21}C_1A \\ i\hbar\dot{C}_3 = \mu_{32}C_2A + \mu_{31}C_1A + C_3E_3 \end{cases} \quad (4)$$

And then the time-dependent population transfer between the spin qubit states will be compared for both cases.

Our goal is to provide an ultrafast transfer of population from one qubit state to another and to establish the regime when the population of the upper level is explicitly equal to zero because of the coherent trapping of population in the two qubit states due to the Raman Λ-type transitions induced by the magnetic field pulse.

Results and Discussion

Ultrafast spin-flip in the case of blocked direct spin transition

First we analyze the possibility of the spin-flip induced by the unipolar magnetic pulse in the case when the direct transition between the qubit spin states is blocked. Under such conditions only Raman Λ-type transitions take place and are responsible for transfer of population from the lower spin state to the upper one.

The system (3) is solved for any instant of time in the time interval $[0, \tau]$ when the magnetic field is turned on and then the field-free dynamics of the system takes place with no change of populations being observed. For convenience we introduce the following notations:

$$E_2 - E_1 = \Delta;\ \ E_3 - E_4 = \Delta_2;\ \ \frac{E_1+E_2}{2} = \bar{E};\quad E_3 - \bar{E} = \hbar\Omega;\quad \mu A = V \tag{5}$$

It should be noticed that since we consider unipolar magnetic pulse which hasn't any carrier frequency, Ω is just a designation.

Then we introduce new variables:

$$\xi(t) = (C_1 + C_2)e^{-\frac{i}{\hbar}\bar{E}t};\ \eta(t) = (C_1 - C_2)e^{-\frac{i}{\hbar}\bar{E}t}\ and\ C(t) = \ C_3 e^{-\frac{i}{\hbar}\bar{E}t} \tag{6}$$

In terms of new variables the system (3) can be rewritten as follows:

$$\begin{cases} i\hbar\dot{\xi} = 2VC - \frac{\Delta}{2}\eta \\ i\hbar\dot{\eta} = -\frac{\Delta}{2}\xi \\ i\hbar\dot{C} = V\xi + C\hbar\Omega \end{cases} \tag{7}$$

The solution of Eq. (7) can be found in the form:

$$\begin{pmatrix} \xi \\ \eta \\ C \end{pmatrix} \sim e^{-\frac{i}{\hbar}\gamma t} \tag{8}$$

where γ is the quasienergy of the system (7) and can be found from the equation:

$$\gamma^2(\gamma - \hbar\Omega) - 2V^2\gamma - \frac{\Delta^2}{4}(\gamma - \hbar\Omega) = 0 \tag{9}$$

Usually for real superconducting systems $\Delta \ll \hbar\Omega$ and the coupling between spin qubit states V induced by magnetic field is rather strong due to huge value of the magnetic dipole moment. For these reasons the Eq. (9) can be solved analytically by sequential iterations and in the limit of $\Delta \to 0$ the following zero-order quasienergies are obtained:

$$\gamma_0^{(0)} = 0;\qquad \gamma_\pm^{(0)} = \frac{\hbar\Omega}{2} \pm \frac{\sqrt{(\hbar\Omega)^2 + 8V^2}}{2} \tag{10}$$

It is interesting to analyze the quasienergy wave function $\psi_{\gamma=0}^{QES}$ corresponding to $\gamma^{(0)} = 0$ which is found to be the following:

$$\psi_{\gamma=0}^{QES} \sim \frac{\varphi_1 - \varphi_2}{\sqrt{2}} \tag{11}$$

Such wave-function corresponds to the case when all the population is trapped in the spin qubit states and the population of the upper state φ_3 is equal to zero. Such regime is referred to as a coherent population trapping known for real atomic systems in optical electromagnetic pulses [29]. If such state is chosen as an initial one, no population of the upper state |3> is detected.

In this paper we consider a qubit system being initially in the lowest state |1> and we are focused on the possible population transfer to the qubit spin state |2>. Using the quasienergies (10) we solve such initial-value problem analytically in the limit of $\Delta \to 0$ and obtain the following time-dependent amplitudes of the considered states

$$C_{1,2}(t) = \pm\frac{1}{2} + \frac{1}{2}e^{-i\frac{\Omega}{2}t}\left[cos\left(\frac{\sqrt{(\hbar\Omega)^2+8V^2}}{2\hbar}t\right) + i\frac{\hbar\Omega}{\sqrt{(\hbar\Omega)^2+8V^2}}\sin\left(\frac{\sqrt{(\hbar\Omega)^2+8V^2}}{2\hbar}t\right)\right] \quad (12)$$

$$C_3(t) = e^{-i\frac{\Omega}{2}t}\frac{V}{\sqrt{(\hbar\Omega)^2+8V^2}}(-2i)\cdot sin\left(\frac{\sqrt{(\hbar\Omega)^2+8V^2}}{2\hbar}t\right) \quad (13)$$

The time-dependent populations of different states obtained from Eqs. (12, 13) are presented at Fig. 2 and are seen to be characterized by very fast oscillations accompanied by rather slow modulation. Fast oscillations correspond to strongly non-resonant Rabi-like transitions between each qubit state and the upper third state that are of great efficiency due to a large value of the magnetic matrix element and therefore a very strong coupling between these levels . And slow modulation represents the transition frequency Ω (or characteristic period $T_\Omega = 2\pi/\Omega$) between the qubit states, or rather, some mean level with energy $\bar{E}$ and the upper third level. It can be seen that the time of the first spin-flip appears to be much shorter than the period T_Ω and further decreases with growing the degree of coupling (for example with the increase of the magnetic field strength, compare Fig. 2a and 2b) since the carrier oscillations become faster. As a result by growing the magnetic field strength it is possible to provide the spin-flip at the ultra-short time scale. For example for $\mu \sim 10^6\ a.u$, $H \sim 5 * 10^{-5}\ a.u$ and $\Omega = 10\text{GHz}$ the characteristic time of the spin transition between the qubit states appears to be about 5 picoseconds what is the record value compared to the nanosecond times achieved for direct Rabi transitions.

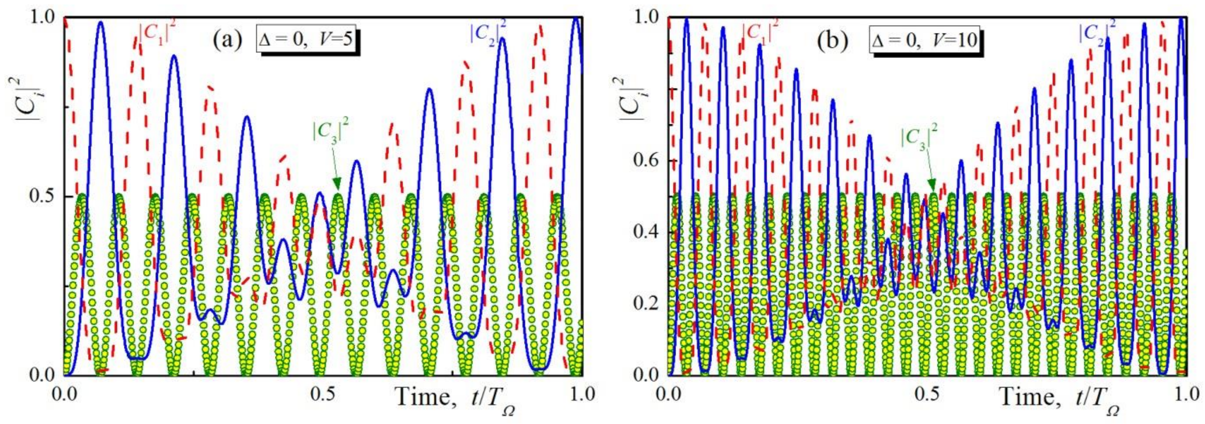

Figure 2: Analytical solution of (7) obtained in the limit Δ→0 for two different magnetic field strengths: V = 5 (a) and V = 10 (b). Dashed lines, solid lines and circles are for $|C_{1,2,3}|^2$ respectively. The decrease of efficiency of the spin transition is prevented by growing the coupling between the spin states.

Let us now discuss the dependence of the spin transition time on the energy distance Δ between the qubit levels. For this goal the solution of (7) was obtained using the quasienergies found from (9) by sequential iterations on the parameter Δ. The obtained analytical solution (they are not presented here due to its complexity) appears to be very close to the explicit numerical results. The dynamics of population of all considered levels obtained for different values of Δ is presented at Fig. 3a. It can be seen that the time of the spin transition is almost the same while the efficiency of transition (maximal achieved population of the second level) decreases with growing Δ (see the inset on Fig. 3b). However the efficiency can be increased by growing the magnetic field impact which provides much faster Rabi-like oscillations and hence almost 100% efficiency of the first peak-population transfer. Thus, while the coupling strength appears to change the carrier frequency of population dynamics, Δ is found to be responsible for the period of slow modulation.

As a result, the characteristic time of the spin flip decreases dramatically with growing the coupling strength without loss of efficiency what is illustrated by Fig. 3b. The time of population transfer (or spin-flip, T_{SF}) is normalized by $T_\Omega = 2\pi/\Omega$. While this period is lying in the sub-nanosecond range the time of the observed spin flip appears to be up to 2 orders of magnitude lower. Thus we really achieve a very quick spin-flip on picosecond times which is dramatically faster than that obtained in the case of carrier magnetic pulse, resonant to the direct transition between spin states.

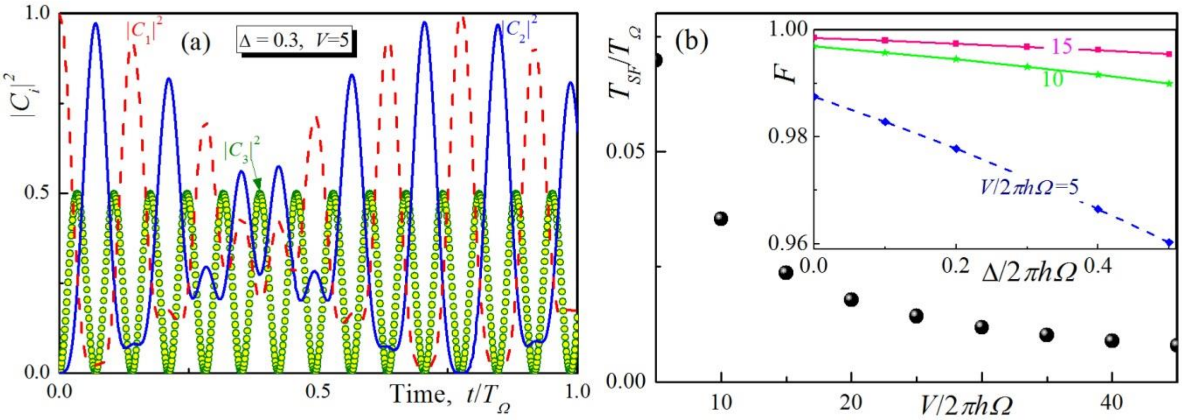

Figure 3: Analytical solution of (7) obtained for Δ=0.3$\hbar\Omega$, V=5, dashed lines, solid lines, circles and squares are for $|C_{1,2,3}|^2$ (a) and the characteristic time of the spin flip versus the degree of coupling between the atom and magnetic field. (b). The time of the spin flip versus the degree of coupling between the atom and magnetic field. The inset shows how the efficiency of the spin-flip operation *F* (determined by $|C_2|^2$ at the first maximum) decreases with increasing normalized value Δ for different coupling V.

Further we have analysed the influence of the additional upper-lying levels of studied superconducting meta-atom on the time of the considered spin-flip. We include a fourth level, which is higher in energy than the third one. The correspondent dynamics of population of different levels is presented at Fig. 4 for coupling parameter V=10. The time of the first peak of the population transfer appears to be even shorter in comparison to the result of Fig. 2b due to the increase of the frequency of slow modulations. Hence the account for the real energy structure of considered superconducting system will not slow down the observed ultrafast spin flip.

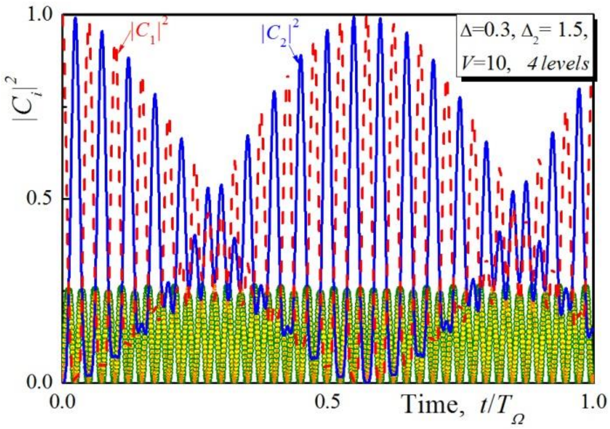

Fig. 4. The time-dependent populations of states calculated when the 4-th upper lying state of the superconducting system is involved in the Raman Λ-type transitions for $\Delta=0.3\hbar\Omega$, $\Delta_2=1.5\hbar\Omega$ and V = 10. Dashed lines, solid lines, circles and squares are for $|C_{1,2,3,4}|^2$ respectively.

Magnetization reversal induced by unipolar magnetic pulse for allowed direct spin transitions

Let's compare the results obtained in the previous section with the case when the direct transition between the spin qubit states |1>→|2> is allowed. Such an unusual situation is possible in an artificial Josephson atom [30]. We will call it the Δ-configuration of a superconducting atom. In this case the system (4) is solved. An analytical expression of the probability amplitude of the upper spin state obtained in the limit of Δ→0 is given by:

$$C_2(t) = -\frac{1}{2}e^{\frac{i}{\hbar}Vt} + \frac{1}{2}e^{-\frac{i(V+\hbar\Omega)t}{2\hbar}}\begin{bmatrix} cos\left(\frac{\sqrt{(V-\hbar\Omega)^2+8V^2}}{2\hbar}t\right) - \\ -i\frac{(V-\hbar\Omega)}{\sqrt{(V-\hbar\Omega)^2+8V^2}}sin\left(\frac{\sqrt{(V-\hbar\Omega)^2+8V^2}}{2\hbar}t\right)\end{bmatrix}, \quad (14)$$

The corresponding dynamics of the population of this state is presented at Fig. 5 for two different values of the magnetic field impact. The result is rather different in comparison with the data of Fig. 2. In contrast to the case when the transition |1>→|2> is blocked now we observe slower spin-flip with the characteristic time determined not by the separation between the spin qubit levels Δ, but by the period $T_\Omega=2\pi/\Omega$ which corresponds to nanosecond or at least to sub-nanosecond time range for real superconducting systems. For this reason the observed spin-flip appears to be significantly faster than in the case of resonant Rabi transitions but dramatically slower than for scheme with blocked direct transition. It should be noticed that the increase of the magnetic field strength (or the coupling between levels) does not influence the characteristic spin-flip time at all.

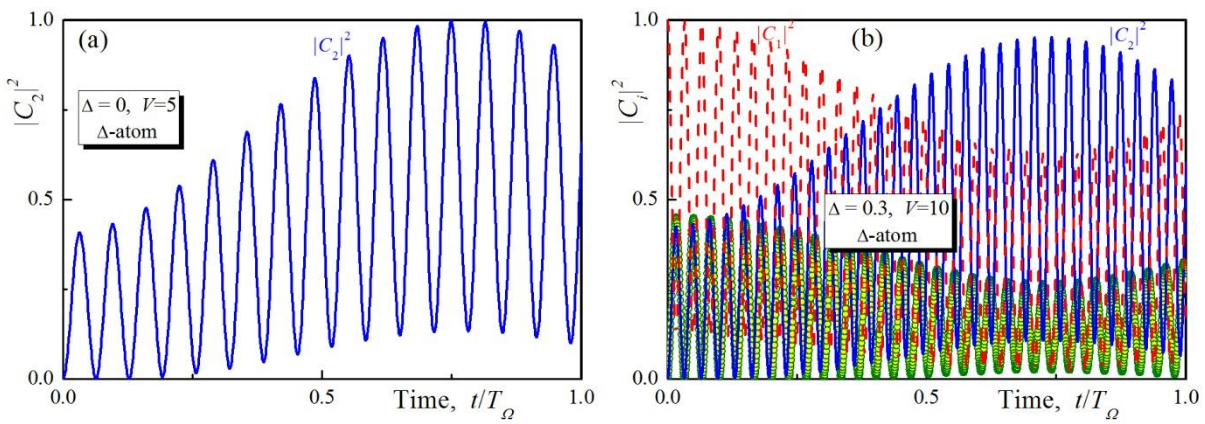

Figure 5: Population of the upper spin state of the superconducting qubit obtained analytically for V = 5 in the limit of Δ→0 (a) and the populations of the all considered states calculated numerically for Δ=0.3$\hbar\Omega$,V = 10 (b). The direct spin transition is allowed. Dashed lines, solid lines and circles are for $|C_{1,2,3}|^2$ respectively.

With the increase of the energy separation between spin states Δ the maximal possible value of the population of the upper spin state starts to decrease which means a drop of transition efficiency, while the characteristic transition time remains almost the same (see Fig. 5b). Thus, in such scheme with the direct spin transition allowed the spin-flip can't be significantly speeded up.

Issues of the experimental realization of the theoretically proposed scheme

First of all, we will demonstrate the possibilities for controlling the distances between energy levels and matrix elements of various transitions in superconducting meta-atoms. For this purposes, we investigated numerically eigenvalues and eigenfunctions of the unperturbed Hamiltonian $\hat{H}_0 = \hat{T}_C + \hat{U}_J$ of the system. Here $\hat{T}_C$ is the Coulomb energy of the system and – $\hat{U}_J$ – Josephson energy. The results of the calculations of the energy eigenvalues and the matrix elements of the operator of the generalized coordinate are presented for different values of the fluxes setting the working point (see Fig. 6). Here, the value Φ_Z determines the potential asymmetry of the potential; the value Φ_X determines parameter α and the size of the barrier between the minima of the potential presented in Figure 1. It can be seen that in a superconducting meta-atom we can really adjust the magnitude of the energy gap and even make it negligible. In addition, we can control the selection rules: there is a range of parameters when, for example, the transition between the lowest energy levels is prohibited.

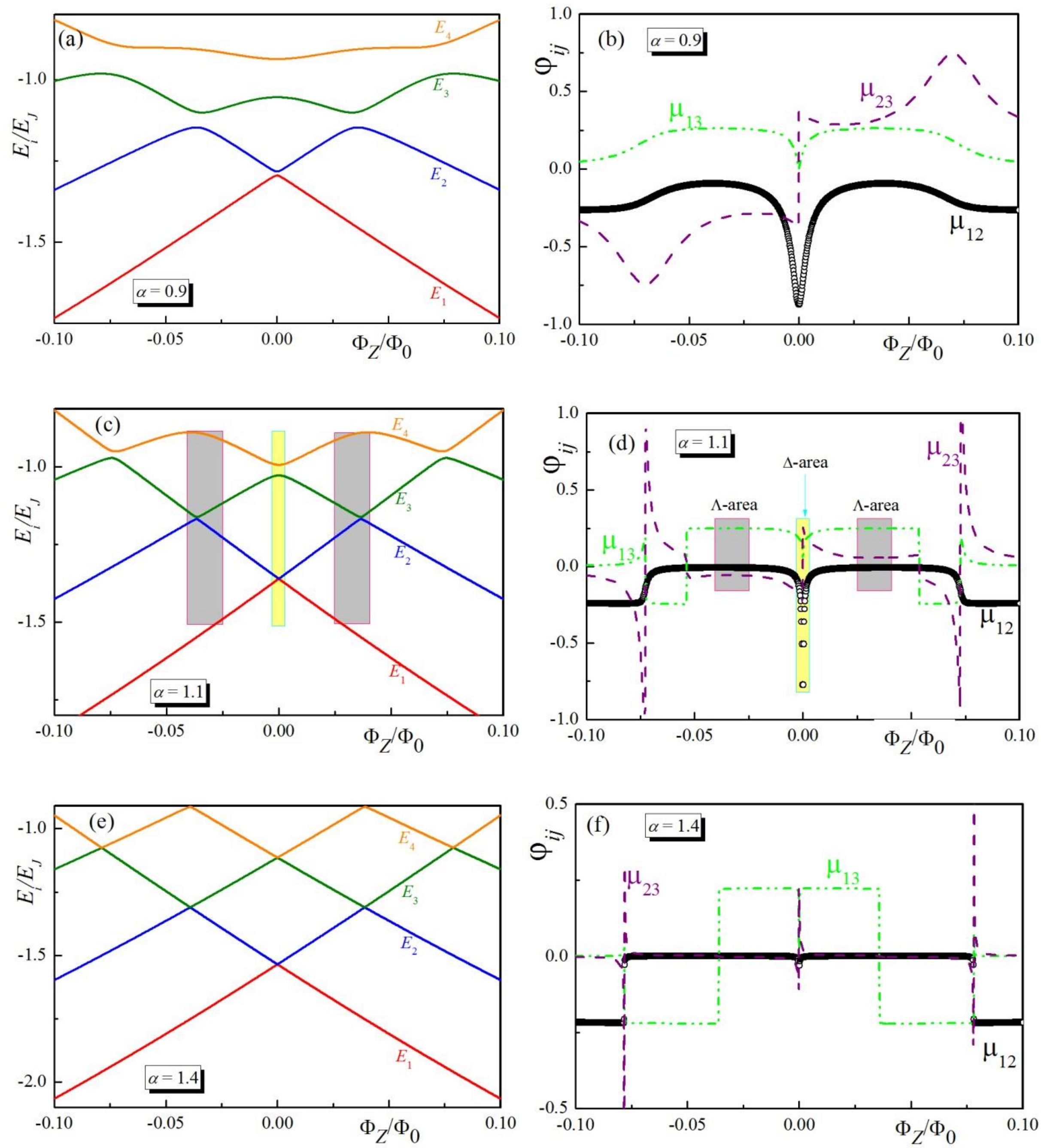

Figure 6: Eigenvalues, $E_{1,2,3,4}$, of the unperturbed Hamiltonian and matrix elements (μ_{ij}) for transitions between its eigenstates for different values of the potential barrier between the wells: α = 0.9 (a, b), α = 1.1 (c, d), and α = 1.4 (e,f).

For small sizes of the potential barrier between minima (for example, $\alpha = 0.9$), the transition between states with energies E_1, E_2 is allowed in a wide range of parameters. For large barriers (α =1.4), transitions are allowed only inside the well. In the intermediate case (α =1… 1.2) there is a mode when the $E_1 - E_2$ transition is prohibited, but $E_1 – E_3$ and $E_3 – E_2$ are allowed (Λ-area). At the figure 8, we have also highlighted the areas of parameters when all three considered transitions are allowed (Δ-area).

An experimental issue of implementation of the proposed picosecond-time qubit control is the difficulties related to generation and application of corresponding picosecond control pulse with minimal parasitic thermal perturbation of the quantum system. The first practical approach in this way dates back to implementation of ballistic fluxon qubit readout [21-28]. The readout design was based on the well-developed Rapid Single Flux Quantum (RSFQ) circuits. Namely, Josephson transmission line realized as a parallel array of lumped Josephson junctions coupled by superconducting inductances was chosen as a control line supporting the flux to be quantized. One cell of the transmission line was magnetically coupled with the qubit so that it was exposed to the magnetic field of the propagating fluxon for a short time. However, an experimental study presented evidence of excessive perturbation of the quantum circuits by this readout scheme.

An improved version of classical interface was proposed in the recent work [19]. Here, the interface circuits devoted to generation and receiving control magnetic flux quanta are implemented on a different chip which is physically located at higher temperature stage in cryocooler. The chips with classical and quantum circuits are connected by using the standard Multi-Chip Module (MCM) technology [31]. Control pulses are propagating in passive transmission lines coupled with qubits in the quantum part of the system. On one hand, such an approach benefits in terms of using standard digital RSFQ circuits for generating the control signal and process the response from quantum circuits while keeping them thermally isolated. On the other hand, the formation of a picosecond control pulse with appropriate parameters becomes a sophisticated problem here which requires advanced rapid-frequency design and was not addressed yet.

A simpler solution could be utilization of Adiabatic Superconducting Logic (ASL) circuits broadly used, e.g., to control qubits in D-Wave Systems quantum processors [32]. While ASL circuits are distinguished by their ultimate energy efficiency, the shape of the magnetic signal transferred by ASL transmission line can be easily tuned in-situ. In comparison with Josephson transmission line, here Josephson junctions are substituted by superconducting adiabatic logic cells [33-36]. This allows you to transfer data not in the form of the presence or absence of quantum, but in the direction of the currents circulating in the superconducting circuits (excluding in the limit the energy dissipation due to the transition in the resistive state). The Figure 7a shows schematically the information transfer in such data bus.

The role of the ASL elements here can be played by connected nSQUIDs - interferometers with a negative mutual inductance of the shoulders [37, 38]. The negative mutual inductance of the shoulders provides: (i) a high inductance for the bias current flowing in the same direction in both shoulders, (ii) a low inductance for the circulating current, which has different signs at the Josephson junctions. The general view and equivalent circuit of such a device are shown in the Figure 7.

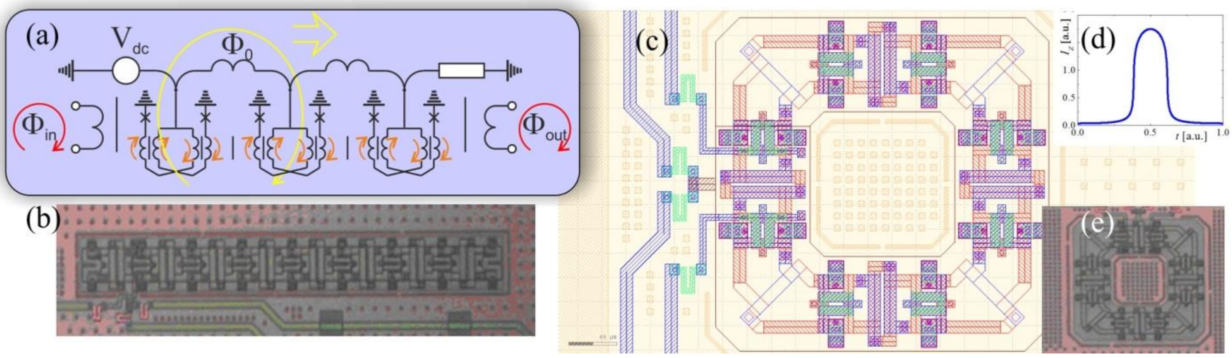

Figure 7: (a) A schematic diagram of a transmission line in ASL-circuits, through which a soliton-like current wave can propagate, creating (from a qubit viewpoint) a control pulse of picosecond duration. Linear (b) and circular (c, e) arrangement of

elements in the experimental implementation for chains of nSQUIDs manufactured by Hypres, as well as the numerically calculated current pulse in the system, whose magnetic field affects the qubit (d).

The sum of the Josephson and inductive energies in the system can be written through the total and difference phases, $\varphi_{\pm}$, of the two Josephson junctions as

$$\frac{2\pi U}{E_J} = \frac{1}{l}\left[\frac{(\varphi_+ - \varphi_c)^2}{1-m} + \frac{(\varphi_- - \varphi_e)^2}{1+m}\right] - 2\cos\varphi_+ \cos\varphi_- , \qquad (15)$$

where *l* and *m* – are the normalized values for the inductance of the shoulder and the mutual inductance correspondingly. A numerical study of the dynamic processes [39] in the nSQUID allowed us to select parameters for which it is possible for the picosecond control pulses to pass through the ASL transmission line. The calculated view of the revisiting control pulse for a qubit is shown in Figure 7d. Particular attention should be paid to the absence of parasitic plasma oscillations of the circuit and field in the optimal mode of operation after carrying out the required impact on the Josephson meta-atom.

Conclusion

In conclusion, in this paper we develop a theoretical concept and its experimental realization of ultrafast switching between selected eigenstates of an artificial atom. The advantage of the proposed scheme consists in usage short unipolar magnetic field pulses which are characterized by significantly broad frequency spectrum. Different spectral components of such broadband pulse can stimulate all possible transitions in the "atomic" system. By blocking the direct transitions between selected states it is possible to controllably transfer the population between them due to Raman Λ-type transitions via upper-lying levels. As a result, the characteristic time of such “non-direct” transitions is found to be on the picosecond scale and appears to be dramatically shorter (several orders of magnitude) than the best values achieved for direct Rabi spin-flip. Up to now in the Rabi-technique using carrier radio pulses with carrier frequency of 0.1 - 100 GHz the achieved reversal times appear to be no shorter than tens of nanoseconds due to small energy separation and near-degeneracy of the spin qubit levels [40]. Such spin-flip time is limited on the one hand by the coherence time (which is no more than 100 μs) and by the inverse frequency of required transition (which is 0.1 – 1 GHz) on the other. In our method the used unipolar pulse has no carrier frequency at all and the time of the induced population transfer determined only by the magnetic field strength and the dipole matrix element of transition can be significantly shortened.

Another key-point of our suggested technique consists in controllable managing the parameters of the experimental scheme with possible blocking the required transitions and smooth adjustment of the energy spectrum and matrix elements to their optimal values found from our theoretical consideration. Switching the regimes from the simple Λ-scheme to the specific case of a Δ-atom is shown and the possibility to fulfill the requirement conditions for the ultrafast control by unipolar picosecond pulses is demonstrated. In addition, in our experimental scheme the parameters of magnetic field can be tuned and optimal magnetic field strength and duration are shown to be reproduced exactly. During the propagation of the soliton-like current wave in the ASL transmission line the magnetic field interacting with the qubit can be represented exactly as required impact. The shape of this pulse can be calculated as convolution of the according function representing the coupling between the qubit and magnetic flux of the vortex in the ASL cell. Thus the shape can be governed *in situ* taking into account the relation between the driving force and losses in the system [24] using the latest advances of superconducting technology.

It should be emphasized that the proposed ultrafast population transfer between selected levels is important not only for the acceleration of the spin-flip transitions in superconducting Josephson qubits, but also play a principal role in ultrafast state initialization for algorithmic quantum computers and quantum neural networks as well as in fast control of the magnetic properties of media from Josephson meta-atoms.

Acknowledgements

We acknowledge partial financial support of the Russian Science Foundation Grant № 19-42-04105 (theoretical approach and calculations) and RFBR Grant № 16-29-09515 (development of circuits for experimental implementation).

References

1. Devoret, M. H.; Schoelkopf, R. J. *Science* **2013**, *339*, 1169-1174.

2. Xiang, Z.-L.; Ashhab, S.; You, J.Q.; Nori F. *Rev. Mod. Phys.* **2013**, *85*, 623.

3. van der Wal, C.H.; ter Haar, A. C. J.; Wilhelm, F. K.; Schouten, R. N.; Harmans, C. J. P. M.; Orlando, T. P.; Lloyd, Seth; Mooij, J. E. *Science* **2000**, *290*, 773-777.

4. Friedman, J. R.; Patel, V.; Chen, W.; Tolpygo, S. K.; Lukens, J. E. *Nature* **2000**, *406*, 43-45.

5. Chiorescu, I.; Nakamura, Y.; Harmans, C. J.; Mooij, J. E. *Science* **2003**, *299*, 1869-1871.

6. Manucharyan, V. E.; Koch, J.; Glazman, L. I.; Devoret, M. H. *Science* **2009**, *326*, 113-116.

7. Steffen, M.; Kumar, S.; DiVincenzo, D.P.; Rozen, J. R.; Keefe, G. A.; Rothwell, M. B.; Ketchen, M. B. *Phys. Rev. Lett.* **2010**, *105*, 100502.

8. Bylander, J.; Gustavsson, S.; Yan, F.; Yoshihara, F.; Harrabi, K.; Fitch, G.; Cory, D.C.; Nakamura, Y.; Tsai, J.; Oliver, W.D. *Nature Physics* **2011**, *7*, 565-570.

9. Grajcar, M.; van der Ploeg, S. H. W.; Izmalkov, A.; Il'ichev, E.; Meyer, H.-G.; Fedorov, A.; Shnirman, A.; Schön, G. *Nature Physics* **2008**, *4*, 612-616.

10. Schoelkopf, R. J.; Girvin S. M. *Nature* **2008**, *451*, 664-669.

11. Izmalkov, A.; van der Ploeg, S. H. W.; Shevchenko, S. N.; Grajcar, M.; Il'ichev, E.; Hübner, U.; Omelyanchouk, A. N.; Meyer, H.-G. *Phys. Rev. Lett.* **2008**, *101*, 017003.

12. Kou, A.; Smith, W. C.; Vool, U.; Brierley, R.T.; Meier, H.; Frunzio, L.; Girvin, S.M.; Glazman, L.I.; Devoret, M.H. *Phys. Rev. X* **2017**, *7*, 031037.

13. F. Tacchino, C. Macchiavello, D. Gerace, and D. Bajoni, An Artificial Neuron Implemented on an Actual Quantum Processor arXiv:1811.02266v1 (2018).

14. Shulga, K. V.; Il'ichev, E.; Fistul, M. V.; Besedin, I. S.; Butz, S.; Astafiev, O.V.; Hubner, U.; Ustinov, A. V. *Nature Communications* **2018**, *9*, 150.

15. Hönigl-Decrinis, T.; Antonov, I. V.; Shaikhaidarov, R.; Antonov, V. N.; Dmitriev, A. Yu.; Astafiev, O. V. *Phys. Rev. A* **2018**, *98*, 041801(R).

16. McDermott, R.; Vavilov, M. G. *Physical Review Applied* **2014**, 2, 014007.

17. Klenov, N.V.; Kuznetsov, A.V.; Soloviev, I.I.; Bakurski, S.V.; Tikhonova, O.V. *Beilstein J. Nanotechnol.* **2015**, 6, 1946.

18. Liebermann, P.J.; Wilhelm, F.K. *Phys. Rev. Applied* **2016**, 6, 024022.

19. McDermott, R.; Vavilov, M. G.; Plourde, B. L. T.; Wilhelm, F. K.; Liebermann, P. J.; Mukhanov, O. A.; Ohki T. A. *Quantum Sci. Technol.* **2018**, 3, 024004.

20. Leonard, E. Jr.; Beck, M. A.; Nelson, J.; Christensen, B.G.; Thorbeck, T.; Howington, C.; Opremcak, A.; Pechenezhskiy, I.V.; Dodge, K.; Dupuis, N.P.; Hutchings, M.D.; Ku, J.; Schlenker, F.; Suttle, J.; Wilen, C.; Zhu, S.; Vavilov, M.G.; Plourde, B.L.T.; McDermott, R. *Phys. Rev. Applied* **2019**, *11*, 014009.

21. Fedorov, A.; Shnirman, A.; Schön, G.; Kidiyarova-Shevchenko, A. *Phys. Rev. B* **2007**, *75*, 224504.

22. Herr (Kidiyarova-Shevchenko), A.; Fedorov, A.; Shnirman, A.; Il'ichev, E.; Schoen, G. *Supercond. Sci. Technol.* **2007**, *20*, S450–S454.

23. Pankratov, A.L.; Gordeeva, A.V.; Kuzmin, L.S. *Phys. Rev. Lett*. **2012**, *109*, 087003.

24. Soloviev, I.I.; Klenov, N.V.; Pankratov, A.L.; Il'ichev, E.; Kuzmin, L.S. *Phys. Rev. E* **2013**, *87*, 060901(R).

25. Fedorov, K. G.; Shcherbakova, A. V.; Schäfer, R.; Ustinov, A. V. *Appl. Phys. Lett.* **2013**, *102*, 132602.

26. Fedorov, K. G.; Shcherbakova, A. V.; Wolf, M.J.; Beckmann, D.; Ustinov, A.V. *Phys. Rev. Lett.* **2014**, *112*, 160502.

27. Soloviev, I.I.; Klenov, N.V.; Pankratov, A.L.; Bakurskiy, S.V.; Kuzmin, L.S. *Appl. Phys. Lett.* **2014**, *105*, 202602.

28. Soloviev, I.I.; Klenov, N.V.; Pankratov, A.L.; Bakurskiy, S.V.; Kuzmin, L.S. *Phys. Rev. B* **2015**, *92*, 014516.

29. Allen, L.; Eberly, J.H. *Optical Resonance and Two-level Atoms* (Dover, New York), 1987.

30. You, J. Q.; Nori, F. *Nature* **2011**, *474*, 589-597.

31. Gupta, D.; Li, W.; Kaplan, S. B.; Vernik, I. V. *IEEE Trans. Appl. Supercond.* **2001**, *11*, 731–734.

32. Johnson, M. W.; Bunyk, P.; Maibaum, F.; Tolkacheva, E.; Berkley, A. J.; Chapple, E. M.; Harris, R.; Johansson, J.; Lanting, T.; Perminov, I. *Supercond. Sci. Technol.* **2010**, *23*, 065004.

33. Takeuchi, N.; Ozawa, D.; Yamanashi, Y.; Yoshikawa N. *Supercond. Science and Techn.* **2013**, *26 (3)*, 035010.

34. Takeuchi, N.; Yamanashi, Y.; Yoshikawa, N. *Supercond. Sci. Technol.* **2015**, 28, 015003.

35. Schegolev, A. E.; Klenov, N. V.; Soloviev, I. I.; Tereshonok, M. V. *Beilstein J. Nanotechnol.* **2016**, *7*, 1397–1403.

36. Soloviev, I. I.; Schegolev, A. E.; Klenov, N. V.; Bakurskiy, S. V.; Kupriyanov, M. Yu; Tereshonok, M. V.; Shadrin, A. V.; Stolyarov, V. S.; Golubov, A. A. *J. Appl. Phys.* **2018**, *124*, 152113.

37. Ren, J.; Semenov, V. K. *IEEE Trans. Appl. Supercond.* **2011**, *21*, 780–786.

38. Averin, D.V.; Xu, K.; Zhong, Y.P.; Song, C.; Wang, H.; Han, S. *Phys. Rev. Lett.* **2016**, *116*, 010501.

39. Soloviev, I.I.; Klenov, N.V.; Bakurskiy, S.V.; Kupriyanov, M.Yu; Gudkov, A.L.; Sidorenko, A.S. *Beilstein J. Nanotechnol.* **2017**, *8*, 2689–2710.

40. Wendin, G. *Rep. Prog. Phys.* **2017**, *80*, 106001.